Motility of Dimeric Ncd on a Metal-Chelating Surfactant: Evidence That Ncd Is Not Processive†

Michael J. deCastro, Chih-Hu Ho, and Russell J. Stewart*

Department of Bioengineering, University of Utah, Salt Lake City, Utah 84112

Received December 10, 1998; Revised Manuscript Received February 11, 1999

ABSTRACT: The surface immobilization methods that allowed single-molecule motility experiments with native kinesin have not worked with the ncd motor protein and other kinesin-related motors. To solve this problem, a surfactant (Pluronic F108) was chemically modified with the metal-chelating group nitrilotriacetic acid (NTA) to allow surface immobilization of histidine-tagged microtubule motors. The chelating surfactant provided a convenient and effective method for immobilization and subsequent motility experiments with a dimeric H-tagged ncd protein (H-N195). In experiments with the absorption of H-N195 to polystyrene (PS) beads coated with F108-NTA, a monolayer of H-N195 bound in the presence of Ni^{2+}, while in the absence of Ni^{2+}, the extent of adsorption of H-N195 to PS beads was greatly reduced. In motility experiments with H-N195 immobilized on F108-NTA-coated surfaces, microtubules moved smoothly and consistently at an average speed of 0.16 ± 0.01 μm/s in the presence of Ni^{2+}, while without Ni^{2+}, no microtubules landed on the F108-NTA-coated surfaces. Investigation of H-N195 motility on the F108-NTA surfaces provided several indications that ncd, unlike kinesin, is not processive. First, a critical H-N195 surface density for microtubule motility of approximately 250 molecules/μm^2 was observed. Second, microtubule landing rates as a function of H-N195 surface density in the presence of MgATP suggested that several H-N195 molecules must cooperate in microtubule landing. Third, the ATP K_M in motility assays (235 μM) was substantially higher than the ATP K_M of dimeric ncd in solution (23 μM) [Foster, K. A., Correia, J. J., and Gilbert, S. P. (1998) *J. Biol. Chem. 273*, 35307−35318].

The kinesin superfamily is a class of motor proteins that convert energy from ATP hydrolysis into movement along microtubules. Since the discovery of the original kinesin (*1*), dozens of kinesin-like proteins have been found that are associated with a wide range of intracellular processes, including vesicle and organelle transport, spindle morphogenesis, and chromosome movements. Members of the kinesin family are defined by a common motor domain with conserved sequence and structure that contains the ATP and microtubule binding sites. Kinesin itself has an N-terminal motor domain and moves toward the microtubule plus end. Other members of the kinesin family, like ncd,[1] have C-terminal motor domains and move toward the microtubule minus end (*2*, *3*).

Several key aspects of kinesin's motility mechanism have been relatively well-characterized using in vitro microtubule motility experiments with surface-immobilized kinesin. The rapid progress was possible, in part, because native kinesin can be nonspecifically adsorbed to glass surfaces in the presence of carrier proteins, like casein, at very low densities of active motors (*4*). Low-surface density motility experiments demonstrated that native kinesin is highly processive; a single kinesin molecule is able to take hundreds of consecutive steps before dissociating from its microtubule track. Using nonspecific adsorption procedures, the magnitude of individual translocation events (*5*) and the forces generated by single native kinesin molecules (*6*−*8*) were measured in high-resolution motility experiments. Other, more specific immobilization procedures have also been developed for genetically truncated kinesin proteins. These procedures include immobilization of in vivo biotinylated kinesin (*9*) and chemically biotinylated kinesin (*10*) on streptavidin-coated surfaces, immobilization of kinesin fused with glutathione *S*-transferase (GST) on surfaces coated with GST antibodies (*11*), and immobilization of kinesin fused with green fluorescent protein (GFP) on surfaces coated with GFP antibodies (*12*).

Unlike kinesin, few details of ncd's motility mechanism are known beyond the direction and speed of movement. Even the question of whether ncd is processive, like kinesin, has not been fully resolved. The difficulty has been that the nonspecific adsorption in the presence of carrier proteins that made motility possible with single native kinesin molecules has not worked well with ncd. Other than the initial reports of ncd minus end-directed motility using the full-length ncd protein expressed in *Escherichia coli* (*2*, *3*), the only ncd motility reported has been with GST and GFP fusion proteins (*11*, *13*−*15*). Likewise, the motility mechanisms of several other kinesin-related proteins, some notoriously reluctant to

† This work was supported by a grant from the NSF to R.J.S. (CTS-9624907), an NIH postdoctoral fellowship to C.-H.H. (HL09777), and a predoctoral Whitaker Foundation Fellowship to M.J.d.

* To whom correspondence should be addressed: Department of Bioengineering, 20S. 2030E., room 506C, University of Utah, Salt Lake City, UT 84112-9458. Phone: (801) 581-8581. Fax: (801) 581-8966. E-mail: rstewart@ee.utah.edu.

[1] Abbreviations: ncd, nonclaret disjunctional; NTA, nitrilotriacetic acid; Pipes, 1,4-piperazinediethanesulfonic acid; IPTG, isopropyl β-D-thiogalactopyranoside; AMPPNP, adenosine 5′-(β−γ-imido)triphosphate; PPO, polypropylene oxide; PEO, polyethylene oxide.

10.1021/bi9829175 CCC: $18.00
Published on Web 04/02/1999

move in vitro, have not been investigated in any detail. A universally applicable method of immobilizing active motors with well-defined densities and with minimal structural modification is needed to resolve the mechanical details of motility by ncd and other kinesin-related motors. To meet this need, we developed a specific immobilization procedure using a metal-chelating Pluronic surfactant that enabled motility experiments with ncd modified only with six terminal histidine residues.

Pluronics are triblock copolymers of two hydrophilic polyethylene oxide (PEO) chains connected by a hydrophobic polypropylene oxide (PPO) chain. The PPO chain of Pluronics adsorbs onto hydrophobic surfaces, while the hydrophilic PEO chains extend into the aqueous phase, creating a protein-repellent interface that prevents nonspecific protein adsorption and denaturation (*16*). To modify Pluronics for immobilization of H-tagged proteins, Pluronic F108 was derivatized with the metal-chelating group nitrilotriacetic acid (NTA) on the terminal hydroxyl groups of the PEO chains to form F108-NTA (*17*). Proteins with genetically added terminal histidine residues have a high affinity for chelated metal ions (*18*). Combining the protein-repellent properties of F108 with the high binding stability of immobilized metal affinity provides a convenient method for surface immobilizing H-tagged recombinant proteins.

Here we report that the chelating F108 Pluronic greatly suppressed nonspecific adsorption of ncd to hydrophobic surfaces in the absence of surface-blocking proteins and allowed consistent and reproducible surface immobilization of H-tagged ncd. Using this immobilization procedure with a structurally well-defined dimeric ncd, the surface density dependence and the ATP dependence of ncd-driven microtubule motility were investigated to address the issue of ncd processivity.

EXPERIMENTAL PROCEDURES

Synthesis of F108-NTA. The synthesis of F108-NTA was carried out as previously described (*17*). Nitrilotriacetic acid (NTA) groups were coupled to the terminal hydroxyl groups of the PEO chains of Pluronic F108 (BASF, Inc., Mount Olive, NJ), creating a metal-chelating Pluronic (F108-NTA).

Construction of pRSET-N195. To construct the pRSET-N195 plasmid, pBS-NCD (*19*) was digested with *Afl*II, blunted with Klenow polymerase, and then digested with *Kpn*I. The resulting fragment was ligated into pRSET B (Invitrogen, Inc., Carlsbad, CA), which had been digested with *Bam*HI, blunted with Klenow polymerase, and then digested with *Kpn*I. The resulting plasmid, pRSET-N195, contains ncd residues K195−K685 and a six-histidine residue tag at the N-terminus. The molecular mass of H-N195, calculated from the amino acid sequence, is 57.5 kDa. The protein expressed by pRSET-N195, except for the histidine tag, is equivalent to the MC1 protein (*13*).

Expression and Purification of H-N195. The recombinant plasmid pRSET-N195 was transformed into *E. coli* strain BL21(DE3) for expression. Single colonies were selected and grown overnight in LB media with 50 μg/mL kanamycin. LB cultures (500 mL) with 50 μg/mL kanamycin were then inoculated at 1:100 with the overnight cultures and grown at 37 °C until mid-log phase. The temperature was lowered to 22 °C, and the cells were induced with 0.1 mM isopropyl β-D-thiogalactopyranoside (IPTG) for 10−12 h. Cells were pelleted by centrifugation (Beckman JA 10 rotor, 4500 rpm for 30 min at 4 °C) and frozen at −70 °C. Frozen cell pellets were resuspended in 5 mL/g lysis buffer [20 mM Hepes (pH 7.0), 150 mM NaCl, 4 mM $MgSO_4$, and 1 mM EGTA] and 100 mg/mL lysozyme and 5 mM phenylmethanesulfonyl fluoride (PMSF) and incubated on ice for 30 min. Lysates were prepared by four cycles of freezing with liquid N_2 and thawing in a 25 °C water bath. After two freeze−thaw cycles, 10 μg/mL DNase I was added and the lysates were incubated on ice for 30 min to reduce the viscosity. After four freeze−thaw cycles, the extract was clarified by centrifugation (Beckman JA 17 rotor, 14 500 rpm for 30 min at 4 °C). The clarified supernatant was mixed with 2 mL of Ni-NTA agarose for 30 min at 4 °C. The column was washed with 50 mL of lysis buffer and then washed again with 50 mL of lysis buffer containing 60 mM imidazole. H-N195 was eluted with 300 mM imidazole. The H-N195 was buffer exchanged into PEM 80 [80 mM Pipes (pH 7.0), 4 mM $MgSO_4$, 1 mM EGTA, and 0.1 mM ATP] using a Sephadex G-25 column. The purity of the H-N195 preparation was determined by SDS−PAGE (Figure 2A). The protein was aliquoted, frozen in liquid N_2, and stored at −70 °C. The concentration of the purified H-N195 was determined using the Bradford method with bovine serum albumin as a standard.

Adsorption of H-N195 onto PS Beads. F108 and F108-NTA (4% w/v) in phosphate buffer (50 mM, pH 7.8) were adsorbed onto PS beads (0.453 μm diameter, 1% w/v) overnight with constant end-over-end mixing at room temperature. The coated beads were then washed by centrifugation to remove unbound F108 and stored in PEM 80 at 4 °C. The F108-NTA beads were charged with Ni^{2+} by incubating the beads in 50 mM $NiSO_4$. The Ni^{2+}-charged beads were then washed by centrifugation to remove excess Ni^{2+} and stored in PEM 80 buffer. The truncated H-tagged H-N195 was incubated with PS beads (0.1% w/w) in PEM 80 with end-over-end mixing at 4 °C. The extent of protein adsorption was determined by pelleting the beads by centrifugation, measuring the protein concentration in the supernatant, and subtracting the supernatant concentration from the initial concentration. H-N195 supernatant concentrations were determined using a Micro BCA protein assay method with bovine serum albumin as a standard.

Equilibrium Sedimentation of H-N195. H-N195 was diluted to a final concentration in PEM 80 containing 0.01 mM ATP. The calculated monomer molecular mass for H-N195 based on the amino acid sequence was 57.5 kDa, including the six histidine residues of the H-tag. Sedimentation equilibrium studies were performed in a Beckman XLA analytical ultracentrifuge using an An-60 Ti rotor. The concentration distribution of H-N195 was permitted to come to equilibrium at three speeds: 12 000, 14 000, and 16 000 rpm. Three H-N195 concentrations were analyzed simultaneously: 1, 0.5, and 0.25 mg/mL. Scans were obtained at 280 nm, and four scans were averaged at equilibrium for each speed. Data analysis was performed using the nonlinear regression program NONLIN (*20*), and the goodness of fit was assessed visually from the residual plots. The Sedimentation equilibrium data were best fit to a single ideal species model with a molecular mass of 108 ± 8 kDa. The calculated molecular mass for a dimer was 115 kDa, suggesting that H-N195 exists as a stable dimer in solution.

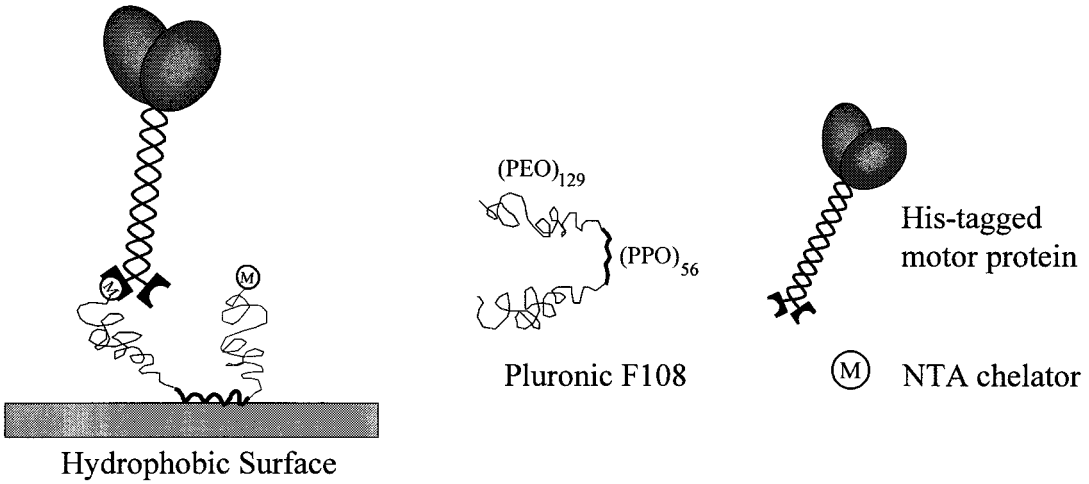

FIGURE 1: Immobilization scheme for histidine-tagged motor proteins using NTA-derivatized Pluronic F108. The hydrophobic PPO block of the Pluronic F108 triblock copolymers interacts with hydrophobic surfaces. The hydrophilic NTA-modified PEO blocks extend into solution, creating an activity-preserving interface to which histidine-tagged proteins bind through chelated metal ions.

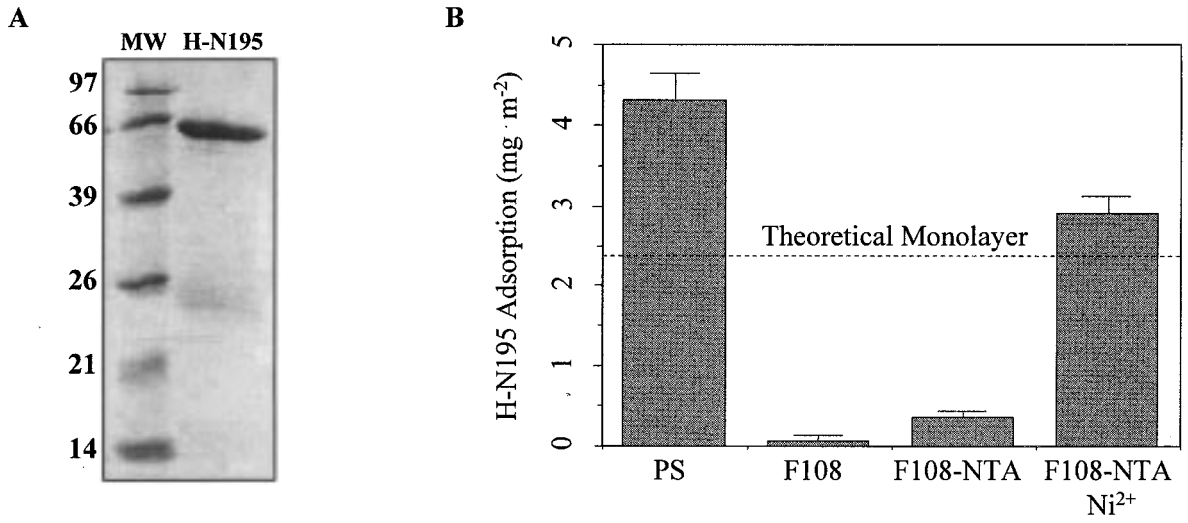

FIGURE 2: H-N195 purification and adsorption on polystyrene (PS) beads. (A) Coomassie-stained SDS−PAGE showing the purity of H-N195 prepared as described in Experimental Procedures. (B) Adsorption of H-N195 on unmodified PS beads and Pluronic-treated PS beads. The dashed line represents a theoretical monolayer of adsorbed N195H on the surface of 0.453 μm PS beads. The values represent the average of at least three protein adsorption measurements. The amount of protein adsorbed onto F108-NTA-treated PS beads in the presence of Ni^{2+} was close to that of the theoretical monolayer (dashed line).

Microtubule Motility and Landing Rate Assays. Flow chambers (24 mm × 5 mm, 12 μL volume) were constructed with a coverslip and a microscope slide separated by two strips of double-stick tape. The coverslips and microscope slides were first treated with dimethyldichlorosilane (DDS) to create hydrophobic surfaces. Dry KOH/EtOH-cleaned surfaces were immersed in 0.05% DDS in trichloroethylene (TCE) for 20 min, washed three times with methanol, washed two times with DI water, dried with filtered air, and stored dry. The DDS flow chambers were incubated with 2 mg/mL F108-NTA and 50 mM Ni^{2+} for 5 min and then washed three times with PEM 80. H-N195 at various concentrations in PEM 80 with ATP or AMPPNP was introduced into the chamber and incubated for 5 min. Finally, microtubules (0.4 μM) in PEM 80, 20 μM taxol, and nucleotide were washed into the flow chamber. Microtubules on the coverslip surface were observed by video-enhanced differential interference contrast microscopy. The density of the motor protein on the DDS coverslip was estimated from the amount of added H-N195, the chamber volume (12 μL), and the area of the glass surfaces of the flow chamber. All the H-N195 was assumed to bind uniformly to the surface of the flow chambers.

RESULTS

Immobilization of H-N195 on F108-NTA. We reported previously that F108-NTA provided a convenient and effective method for immobilizing H-tagged firefly luciferase on PS beads while retaining high specific activity (*17*). The adsorption of histidine-tagged ncd to PS beads treated with F108 and F108-NTA was similarly examined (Figure 2). The ncd protein used for these experiments, designated H-N195, contains the entire predicted coiled coil of ncd and an amino-terminal histidine tag. Analysis of the molecular mass by sedimentation equilibrium demonstrated that H-N195 is dimeric, as expected, and behaves as a single species (data not shown). The amount of H-N195 adsorbed onto PS beads was estimated by subtracting the amount of H-N195 in the

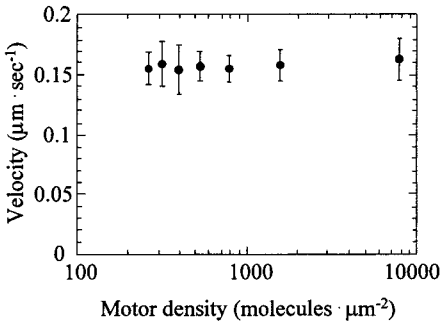

FIGURE 3: Microtubule gliding velocity on different surface densities of H-N195. Each data point represents the average speed of at least five microtubules. In the presence of Ni^{2+} ions, the microtubule gliding velocity (0.16 ± 0.01 μm/s) is independent of H-N195 surface density above a critical surface density of approximately 250 motors/μm^2. In the absence of Ni^{2+}, no microtubules were observed to land on the flow chamber surface even in the presence of MgAMPPNP and at the highest motor concentrations.

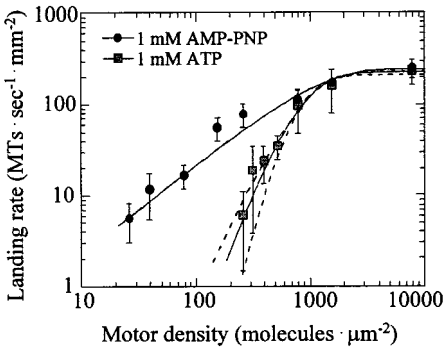

FIGURE 4: Rates of microtubules landing on a H-N195-coated surface in the presence of 1 mM MgATP (■) and 1 mM MgAMPPNP (●). H-N195 molecules were immobilized on F108-NTA-Ni^{2+}-coated DDS coverslips. Each data point represents data from at least six different assays. In the presence of MgAMPPNP, the landing curve was fit when $n = 1$ (± 0.167), while in the presence of MgATP, the landing curve was fit when $n = 4$ (± 0.746), which implies cooperative binding. Also shown are MgATP data fits when $n = 3$ and 7 (dashed lines).

supernatant after the beads were pelleted from the total amount of H-N195 incubated with the PS beads. The estimated mass of adsorbed H-N195 was compared to the theoretical mass of a monolayer of H-N195 (Figure 2, dashed line), calculated from the dimensions (70 Å × 45 Å × 45 Å) of the motor domain crystal structure (*21*) and the surface area of 0.453 μm diameter PS beads. The model assumed the dimeric motor was oriented with its heads projecting away from the bead, as shown in Figure 1, and that the motor domains of the dimer occupied a circular cross-sectional area with a radius of 45 Å.

Untreated PS beads adsorbed 4.33 ± 0.32 mg/m^2 of H-N195, significantly greater than that of the predicted monolayer. The excessive adsorption may have been due to tighter packing of randomly oriented, nonspecifically bound dimeric motors, or multiple layers of adsorbed protein. Beads coated with F108 and F108-NTA in the absence of Ni^{2+} ions, on the other hand, adsorbed much less H-N195 (0.09 ± 0.06 and 0.38 ± 0.05 mg/m^2, respectively), which demonstrated that F108 effectively reduced the level of nonspecific protein adsorption to PS beads. In the presence of Ni^{2+} ions, F108-NTA-coated PS beads adsorbed 2.93 ± 0.21 mg/m^2 of H-N195, slightly more than the theoretical monolayer. The substantial increase in the amount of H-N195 adsorbed to F108-NTA-treated PS beads in the presence of Ni^{2+} ions demonstrated that H-N195 was bound specifically through the H-tag in a manner consistent with the assumptions of the oriented monolayer model. Similar experiments have been carried out with H-tagged kinesin proteins with similar results (not shown).

Microtubule Motility on F108-NTA Surfaces. To use the F108-NTA for standard microtubule motility experiments, glass slides and coverslips were silanized with dichlorodimethylsilane (DDS) to create hydrophobic surfaces. Flow chambers assembled with the DDS glass were coated with F108-NTA in the presence and absence of Ni^{2+} ions, and then incubated with H-N195. In the presence of Ni^{2+} ions and 1 mM MgATP, microtubules moved smoothly and consistently with an average speed of 0.16 ± 0.01 μm/s (Figure 3). In the absence of Ni^{2+} ions, no microtubules were observed to land on the flow chamber surface in the presence of either MgATP or MgAMPPNP even after incubation of the flow chambers with high concentrations of ncd motor. The F108-NTA, therefore, provided an effective method for surface immobilizing ncd for in vitro motility experiments in the absence of carrier proteins and without being fused to GST or GFP.

The speed of microtubule movement on the F108-NTA-Ni^{2+} surfaces was independent of H-N195 density down to a threshold density of approximately 250 motors/μm^2; below the threshold motor density, no microtubule landing or motility occurred (Figure 3). In MgAMPPNP, microtubules landed on the surface at H-N195 densities of <20 motors/μm^{-2}, which demonstrated the presence of active H-N195 on the flow chamber surface. The threshold surface density for microtubule motility in MgATP is in sharp contrast to results from similar experiments with native kinesin (*4*) in which microtubule landing and motility were observed at surface densities of <10 motors/μm^2, surface densities where microtubules moved on single kinesin motors. The threshold density for H-N195 motility was consistent with our previous report that single dimeric ncd motors, in contrast to dimeric kinesin, are not capable of sustained microtubule movement (*14*).

H-N195 Density Dependence of the Microtubule Landing Rate. The critical surface density required for H-N195 motility suggested that multiple H-N195 motors were necessary for sustained microtubule movement that can be observed in a standard motility assay. To estimate the number of dimers that are necessary for motility, the rate of microtubule binding to H-N195 surfaces was determined over a range of H-N195 surface densities (Figure 4). The microtubule landing rate is proportional to the probability that a microtubule will contact simultaneously the threshold number of H-N195 motors. The probability of at least one motor being within the surface area contacted by the microtubule, from the Poisson distribution function, is given by the equation $1 - e^{-\rho/\rho_0}$, where ρ is the density of motors and ρ_0 is the area effectively occupied by a single motor, the area over which a motor can bind a microtubule (*22*). If several ncd dimers must cooperate for a microtubule to land, then the microtubule landing curve should have a general power law dependence on the probability of a single motor

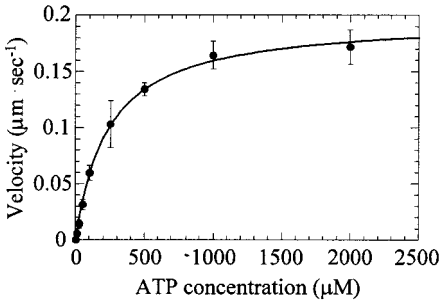

FIGURE 5: Microtubule gliding velocity as a function of ATP concentration. The H-N195 surface density was approximately 1500 motors/μm^2. Each data point represents the average speed of at least five microtubules. The data were fit (solid line) to the Michaelis−Menten equation with a V_{max} of 0.189 ± 0.002 μm/s and a K_{M-ATP} of 235 ± 16 μM.

interacting with a microtubule, $(1 - e^{-\rho/\rho_0})^n$, where n is a Hill-like coefficient that gives an estimate of the number of motors that cooperate in microtubule landing and motility (*22*). In the presence of 1 mM MgATP, the microtubule landing rate was constant at approximately 300 microtubules s^{-1} mm^{-2} above a surface density of about 1500 molecules/μm^2. At H-N195 surface densities of <1500 molecules/μm^2, the landing rate decreased with the H-N195 surface density until no landing was observed below about 250 molecules/μm^2. The best fit to the landing curve in a log−log plot was 4, which implied that four H-N195 dimers cooperate in microtubule landing and stable motility. For comparison, fits with slopes of 3 and 7 are also shown (Figure 4, dashed lines).

The nonhydrolyzable ATP analogue, AMPPNP, induces a tight binding, rigor-like state in ncd. To validate the experimental procedure for determining the power law dependence of microtubule landing rates on the H-N195 surface density, the landing rates were determined in the presence of MgAMPPNP. Because a single dimeric ncd binds tightly to microtubules in the presence of MgAMPPNP, noncooperative microtubule landing by H-N195 was expected. Consistent with this expectation, in the presence of MgAMPPNP, the log−log microtubule landing rate curve was best fit when $n = 1$ (Figure 4).

ATP Dependence of H-N195 Motility. The speed of H-N195-driven microtubule motility was investigated as a function of ATP concentration at a surface density of 1500 motors/μm^2 (Figure 5). The ATP dependence of the motility speed was fit well by the Michaelis−Menten equation with a V_{max} of 0.189 μm/s and a K_{M-ATP} of 235 μM. For comparison, the K_{M-ATP} for dimeric ncd in solution is approximately 23 μM (*23*).

DISCUSSION

Surface Immobilization and Motility of Dimeric Ncd. The metal-chelating F108-NTA reagent provided a convenient and effective method for immobilizing H-tagged ncd proteins. To prepare a stable, activity-preserving surface for ncd motility experiments, the reagent was simply adsorbed onto silanized glass slides and coverslips. This method can be easily applied to submicron polystyrene or glass beads for high-resolution motility experiments using instrumentation based on optical tweezers. Because the Pluronic foundation is oriented on the hydrophobic surface and the motor is bound through terminal histidine residues, the mechanical linkage between the motor and the surface is defined and consistent. And since the attachment is chemically defined, it may be possible to adjust the linkage compliance between the motor protein and surface by using a Pluronic with shorter or longer PEO blocks. In single-molecule, micromechanical experiments with optical tweezers, the consistent linkage compliance will allow direct comparison between individual protein molecules, as well as direct comparisons between various recombinant forms of kinesin motors, single-headed derivatives of kinesin and ncd for example. We have observed motility similar to that reported here with several other H-tagged truncations of both ncd and kinesin (unpublished observations). Since the attachment method has worked with several H-tagged proteins, it may be generally applicable to other H-tagged kinesins, including those that have not yet moved, like MCAK and XCMK (*24*, *25*), allowing direct comparisons of motility data between kinesin family members.

Processivity of Dimeric Ncd. Highly processive motility is a hallmark feature of kinesin. Whether processivity is a common feature of the kinesin family of motors has not been fully answered, although evidence that ncd is not as processive as kinesin has been previously reported (*12*, *14*). The microtubule landing and motility data we report provided additional indications that multiple ncd dimers are necessary for sustained microtubule motility and therefore ncd is not processive in the same way as kinesin. The first indication was the critical surface density of H-N195 required for microtubule motility (Figure 3). At densities below about 250 motors/μm^2, microtubules did not land on the surface, although active motors were present on the surface since microtubules were reversibly bound in the presence of MgAMPNP. Single molecules of dimeric ncd are not capable of sustaining observable microtubule movements even with low concentrations of ATP.

Comparing the maximum rate of ncd-driven microtubule motility in vitro to the maximum rate of microtubule-activated ATP hydrolysis in solution provides a second indication of low ncd processivity. The maximum motility speed of about 160 nm/s corresponds to 20 tubulin subunits/s, or 20 motor binding sites spaced at 8 nm intervals along a single microtubule protofilament. The k_{cat} for ATP hydrolysis by dimeric ncd in solution is 2 s^{-1} per motor domain, or 4 s^{-1} per ncd dimer (*23*). That means that five tubulin subunits (40 nm) must pass by a stationary dimeric motor for each ATP that is hydrolyzed by the dimer. In other words, even if ncd is weakly processive in the hand-over-hand manner widely accepted for kinesin, taking a minimum of two concerted steps, then at 4 steps/s the ncd dimer will be strongly bound to the microtubule for 0.5 s, during which time the microtubule was observed to move 80 nm. Ncd either takes very large steps (40 nm), hydrolyzes ATP much faster in the motility assay than in solution, or is not even weakly processive.

The critical surface density for motility implied that several ncd dimers must cooperate during sustained microtubule movement. To estimate the minimum number of ncd dimers that cooperate in microtubule movement, we determined the H-N195 surface density dependence of the microtubule landing rate. If multiple motors are necessary, then at low surface densities the landing rate should have a power law

dependence on the motor surface density with the exponent being equal to the number of cooperating motors (*22*). On the other hand, if a single motor is sufficient, then at low motor densities there should be a linear dependence of the microtubule landing rate on the motor surface density. In the presence of MgATP, the curve of the log−log binding curve was best fit when $n = 4$, which suggested that at least four dimeric ncds are necessary for a microtubule to land and move in the presence of MgATP. To validate the experimental approach under conditions in which a single dimeric ncd is sufficient for a microtubule to land, the microtubule landing curve was determined in the presence of MgAMPPNP. As expected, a curve when $n = 1$ was the most accurate representation of the data.

The stochastic molecular motor model of Leibler and Huse (*26*) predicts that the ratio of the K_{M-ATP} for filament-activated ATP hydrolysis in solution and the K_{M-ATP} for motility is approximately equal to the number of motors necessary to saturate the rate of filament motility, which is equivalent to the minimum number of motors necessary for sustained filament motility. For nonprocessive skeletal muscle myosin, the K_{M-ATP} for motility with dimeric myosin was reported to be 60 μM and for ATP hydrolysis in solution 4 μM (*27*). The myosin K_{M-ATP} ratio (15) and the corresponding duty ratio (0.07) are in good agreement with experimental measurements of myosin duty ratios (*28*, *29*) in support of the Leibler−Huse model. Likewise, for highly processive kinesin, the K_{M-ATP} ratio was approximately 1 (*30*), as predicted by Leibler and Huse. For H-N195, the K_{M-ATP} for motility, 235 μM (Figure 4), was 10-fold higher than the reported K_{M-ATP} for ATP hydrolysis in solution by dimeric ncd, 23 μM (*23*). The ncd K_{M-ATP} ratio suggests that about 10 motors, or 5 ncd dimers, work together to sustain microtubule movement at the maximum rate in the motility assay.

The processivity or nonprocessivity of ncd has important implications for models accounting for the opposite direction of movement of ncd and kinesin on microtubules. In positional bias models for direction (*31*, *32*), the unbound motor domain of a microtubule-bound dimer is positionally constrained toward the direction of movement by the bound motor domain. Processivity is an implicit requirement of this model; a strong binding state between force-generating states is necessary to constrain the position of the unbound motor domain. The most straightforward interpretation of our data, however, is that ncd is not even weakly processive in the hand-over-hand manner of kinesin. One possibility that would reconcile nonprocessivity and the positional bias model is that the two motor domains of the ncd dimer may cooperate in taking a single 8 nm step; binding by the first motor domain may position the second motor domain for a single binding and force-generating event resulting in an 8 nm step, which is immediately followed by release of the dimer from the microtubule. Fully resolving these issues will require experiments using optical tweezer-based instrumentation capable of resolving unitary translocation events by individual motors. Such experiments are in progress with dimeric ncd.

ACKNOWLEDGMENT

We thank Christoph Schmidt for many helpful discussions and Loren Limberis for comments on the manuscript.

REFERENCES

Vale, R. D., Reese, T. S., and Sheetz, M. P. (1985) *Cell 42*, 39−50.
Walker, R. A., Salmon, E. D., and Endow, S. A. (1990) *Nature 347*, 780−782.
McDonald, H. B., Stewart, R. J., and Goldstein, L. S. (1990) *Cell 63*, 991−1000.
Howard, J., Hudspeth, A. J., and Vale, R. D. (1989) *Nature 342*, 154−158.
Svoboda, K., Schmidt, C. F., Schnapp, B. J., and Block, S. M. (1993) *Nature 365*, 721−727.
Svoboda, K., and Block, S. M. (1994) *Cell 77*, 773−784.
Meyhöfer, E., and Howard, J. (1995) *Proc. Natl. Acad. Sci. U.S.A. 92*, 574−578.
Hunt, A. J., Gittes, F., and Howard, J. (1994) *Biophys. J. 67*, 766−781.
Berliner, E., Mahtani, H. K., Karki, S., Chu, L. F., Cronan, J. E., and Gelles, J. (1994) *J. Biol. Chem. 269*, 8610−8615.
Inoue, Y., Toyoshima, Y. Y., Iwane, A. H., Morimoto, S., Higuchi, H., and Yanagida, T. (1997) *Proc. Natl. Acad. Sci. U.S.A. 94*, 7275−7280.
Stewart, R. J., Thaler, J. P., and Goldstein, L. S. B. (1993) *Proc. Natl. Acad. Sci. U.S.A. 90*, 5209−5213.
Case, R. B., Pierce, D. W., HomBooher, N., Hart, C. L., and Vale, R. D. (1998) *Cell 90*, 959−966.
Chandra, R., Salmon, E. D., Erikson, H. P., Lockhart, A., and Endow, S. A. (1993) *J. Biol. Chem. 268*, 9005−9013.
Stewart, R. J., Semerjian, J., and Schmidt, C. F. (1998) *Eur. Biophys. J. 27*, 353−360.
Allersma, M. W., Gittes, F., deCastro, M. J., Stewart, R. J., and Schmidt, C. F. (1998) *Biophys. J. 74*, 1074−1085.
Andrade, J. D., Hlady, V., and Jeon, S. I. (1996) *Adv. Chem. 248*, 51.
Ho, C. H., Limberis, L., Caldwell, K. D., and Stewart, R. J. (1998) *Langmuir 14*, 3889−3894.
Porath, J., Carlsson, J., Olsson, I., and Belfrage, G. (1975) *Nature 258*, 598−599.
McDonald, H. B., and Goldstein, L. S. (1990) *Cell 61*, 991−1000.
Johnson, M. L., Correia, J. J., Yphantis, D. A., and Halvorson, H. R. (1981) *Biophys. J. 36*, 575−588.
Sablin, E. P., Kull, F. J., Cooke, R., Vale, R. D., and Fletterick, R. J. (1996) *Nature 380*, 555−559.
Hancock, W. O., and Howard, J. (1998) *J. Cell Biol. 140*, 1395−1405.
Foster, K. A., Correia, J. J., and Gilbert, S. P. (1998) *J. Biol. Chem. 273*, 35307−35318.
Wordeman, L., and Mitchison, T. J. (1995) *J. Cell Biol. 128*, 95−105.
Walczak, C. E., Mitchison, T. J., and Desai, A. (1996) *Cell 84*, 37−47.
Leibler, S., and Huse, D. A. (1993) *J. Cell Biol. 121*, 1357−1368.
Harada, Y., Noguchi, A., Kishino, A., and Yanagida, T. (1987) *Nature 326*, 805−808.
Uyeda, T. Q. P., Kron, S. J., and Spudich, J. A. (1990) *J. Mol. Biol. 214*, 699−710.
Finer, J. T., Simmons, R. M., and Spudich, J. A. (1994) *Nature 368*, 113−119.
Wei, H., Young, E. C., Fleming, M. L., and Gelles, J. (1997) *Nature 388*, 390−393.
Hirose, K., Lockhart, A., Cross, R. A., and Amos, L. A. (1996) *Proc. Natl. Acad. Sci. U.S.A. 93*, 9539−9544.
Sablin, E. P., Case, R. B., Dai, S. C., Hart, C. L., Ruby, A., Vale, R. D., and Fletterick, R. J. (1998) *Nature 395*, 813−816.

BI9829175